applied microbiology

MDPI

Article

Genomic Features of *Pseudomonas putida* PCL1760: A Biocontrol Agent Acting via Competition for Nutrient and Niche

Daniel Mawuena Afordoanyi [1,2,*], Roderic Gilles Claret Diabankana [1,3], Aynur Kamilevich Miftakhov [1], Evgenii Sergeyevich Kuchaev [1] and Shamil Zavdatovich Validov [1,*]

[1] Laboratory of Molecular Genetics and Microbiology Methods, Kazan Scientific Center, Russian Academy of Sciences, 420111 Kazan, Russia
[2] Kazan Institute of Biochemistry and Biophysics, Kazan Scientific Center, Russian Academy of Sciences, 420111 Kazan, Russia
[3] Centre of Agroecological Research, Kazan State Agrarian University, 420015 Kazan, Russia
* Correspondence: d.afordoanyi@knc.ru (D.M.A.); szvalidov@kpfu.ru (S.Z.V.)

Abstract: *Pseudomonas putida* strain PCL1760 is a biocontrol agent protecting plants from pathogens via the mechanism of competition for nutrients and niches (CNN). To confirm this mechanism as well as to adapt the strain for biotechnological applications, full genome analysis was compared with the known biotechnological model, *P. putida* S12, and other related species, which were analyzed on different genomic databases. Moreover, the antibacterial activity of PCL1760 was tested against *Staphylococcus aureus*, *Pseudomonas aeruginosa*, and *Pseudomonas syringae*. No genetic systems involved in antibiosis were revealed among the secondary metabolite clusters of the strain of PCL1760. The only antagonistic effect was observed against *P. syringae*, which might be because of siderophore (yellow-greenish fluorescence), although less than 19% pyoverdin biosynthesis clusters were predicted using the AntiSMASH server. *P. putida* PCL1760 in comparison with the *Pseudomonas simiae* strain PCL1751, another biocontrol agent acting solely via CNN, which lost its 'luxury' genes necessary for antibiosis or parasitism/predation mechanisms, but carries genetic systems providing motility. Interestingly, immunity genes (CRISPR/Cas and prophages) showed PCL1760 to be robust in comparison with S12, while annotation on OrthoVenn2 showed PCL1760 to be amenable for genetic manipulations. It is tempting to state that rhizobacteria using the mechanism of CNN are distinguishable from biocontrol agents acting via antibiosis or parasitism/predation at the genomic level. This confirms the CNN of PCL1760 as the sole mechanism for biocontrol and we suggest the strain as a new model for genetic engineering.

Keywords: *Pseudomonas putida* PCL1760; biocontrol; nutrient competition; antagonism; full-genome; prophage; CRISPR/Cas; antimicrobial resistant genes

Citation: Afordoanyi, D.M.; Diabankana, R.G.C.; Miftakhov, A.K.; Kuchaev, E.S.; Validov, S.Z. Genomic Features of *Pseudomonas putida* PCL1760: A Biocontrol Agent Acting via Competition for Nutrient and Niche. *Appl. Microbiol.* **2022**, *2*, 749–765. https://doi.org/10.3390/applmicrobiol2040057

Academic Editor: Alessandro Vitale

Received: 10 September 2022
Accepted: 28 September 2022
Published: 2 October 2022

1. Introduction

Biological control of plant disease has been considered the safest method for controlling plant diseases considering the harmful effects of chemical application such as fungicides and antibiotics on the ecology as a whole. The effectiveness of biocontrol agents varies (30–100%) in comparison with commercial fungicides, which is almost completely effective because of diverse environmental conditions, different strains of pathogens, and the inconsistency of biocontrol strains [1]. The mechanisms for biocontrol of plant pathogens to date include the production of antimicrobial compounds (antibiosis), the induction of plant resistance (induced systemic resistance (ISR), parasitism and predation based on the secretion of hydrolytic enzymes for the consumption of lysed cells of the pathogens, competition for plant nutrients and niches (CNN), and interference with pathogenicity factors of the pathogen [2]. The effective genera of rhizobacteria with these mechanisms mostly include *Pseudomonas* and *Bacillus* [3].

Pseudomonas putida is one of the ubiquitous species found in soils, plants, and waterbodies with a wide application in both the agricultural and industrial sectors. Their ability to control phytopathogens such as *Fusarium oxysporum*, *Xanthomonas campestris*, *Rhizoctonia solani*, *Colletotrichum gloeosporioides*, *Athelia rolfsii*, *Gibberella moniliformis Magnaporthe oryzae*, *Ralstonia pseudosolanacearum*, and plant parasitic nematode *Radopholus similis* has been well documented in several scientific works [4–6]. As a plant growth-promoting bacteria, *P. putida* strains have been known to produce the phytohormone, indoleacetic acid (IAA) [7], as well as solubilize phosphate [8] and fix nitrogen [9].

The use of *P. putida* as a cell factory in bio-industrial applications, through its genomic engineering amenability, its robustness to extreme conditions, and fast growth in minimal medium, has revolutionized the production of beneficial compounds [10]. Since its discovery, *P. putida* has also been adapted for the degradation of toxic compounds, which include aliphatic, aromatic, and heterocyclic compounds [11]. Other applications include the decolorization of dyes by peroxidases used in biosensors or immunodetection analysis [12] and, recently, *P. putida* was applied in the degradation of ceftriaxone through genetic engineering [13]. Another recent work is the treatment of diazinon in wastewater by the popular *P. putida* KT2440 [14].

P. putida strain PCL1760 was isolated from the rhizosphere of an avocado plant and has been proven to control *Fusarium oxysporum* f. sp. *radicis-lycopersici* ZUM2407 via the mechanism "competition for nutrients and niches" (CNN) [15]. Taking into account the diverse abilities of *P. putida* strains [16], strain PCL1760 may possess other mechanisms besides CNN to control plant diseases. To confirm this mechanism and the propensity of PCL1760 to be used as a model for genetic manipulations in biotechnological applications, the full genome needs to be analyzed and compared with other closely related species. We compared the full genetic sequence of *P. putida* PCL1760 to *P. putida* S12 as well as to other different species: *P. simiae* PCL1751, *P. simiae* WCS417, *P. flourescens* W-6, and *P. flourescens* Pt14. We further confirmed its antagonistic activity on bacterial pathogens to prove CNN the as sole mechanism of biological control for *P. putida* PCL1760.

2. Materials and Methods

Complete genomes used in this study were obtained from NCBI genomes (Table 1).

Table 1. Genomes used in this study.

Microbial Strains	NCBI GenBank	Source of Isolation	Reference
P. putida PCL1760	CP099727.1	From the rhizosphere of the avocado plant	In this study
P. simiae PCL1751	NZ_CP010896.1	From the rhizosphere potato	Kamilova et al. [17]
P. fluorescens Pt14	CP017296.1	From the rhizosphere of rice plants in acidic soil	Rani et al. [18]
P. simiae WCS417	NZ_CP007637.1	From lesions of wheat roots growing in a take all disease-suppressive soil	Pieterse et al. [19]
P. putida S12	CP009974.1	From soil using styrene as a sole carbon source	Hartmans et al. [20]
P. fluorescens W-6	CP058533.1	From the Napahai plateau wetland	Xiang et al. [21]

2.1. Genomic DNA Preparation

Chromosomal genomic DNA of *P. putida* PCL1760 was extracted using TRIzol reagent (Thermo Fisher, Waltham, MA, USA) according to the manufacturer's protocol, from the pellet of overnight culture grown at 28 °C in King's B (KB) medium (g/L: 10 g proteose peptone, 1.5 g K_2HPO_4, 15 g glycerol, 1.5 g $MgSO_4$, pH 7.2).

2.2. Library Preparation, Genome Sequencing, and Annotation

The DNA library for bacterial genome sequencing was prepared from high-quality genomic DNA. The whole genome of *P. putida* PCL1760 was sequenced using paired-end

(PE) 2 × 125 bp on the MiSeq Illumina® platform at Evrogen (Moscow, Russia). The quality of raw sequence data was analyzed using FastQC (v. 0.11.2) [22]. To remove adapters and low-quality reads, the sequencing reads were trimmed using Trimmomatic v. 0. 36 [23]. The high-quality adapter-free reads were then de novo assembled using the Unicycler v. 0.5.0 [24], while contigs with size < 200 bp or coverage lower than 10× were cut from the genome assembly. Average nucleotide identity based on Blast (ANIb) was used to select the closely related reference strain by measuring nucleotide level similarity between the coding regions of the genomes with those of NCBI. Mauve Contig Mover [25] was then used to align and reorder contigs based on comparison with the complete reference genome. The quality of the assembled genomes was evaluated using QUAST [26]. Gaps within the scaffolds were filled and closed using GAPPadder, v. 1.10 [27]. The assembled genome sequence of PCL1760 was deposited in NCBI GenBank under the accession number CP099727.1.

2.3. Genome Annotation and Comparison

The genome annotation of *P. putida* PCL1760 was carried out using the Prokaryotic Genome Annotation Pipeline (PGAP) provided by NCBI [28]. The coding gene prediction of the genome was also performed with Prokka (rapid prokaryotic genome annotation) version 1.12 [29].

Pan-genome analysis based on Roary (which takes the GFF3 file of the annotated assemblies produced by Prokka) [30] with default parameters was used to compare the genomic relationships between PCL1760 and the selected genomes. Whereas more than 95% identical genes' prevalence in all genomes (>99%) of the compared strain are classified as Core genes, Cloud genes refers to gene families present only in one genome and Shell genes refer to gene families present in two genomes. OrthoVenn2 was applied for whole genomic comparison and annotation of orthologous clusters [31]. We further used the BlastN search method to screen for the presence of genes involved in the production of functional flagella (*FlgK*, *FlgL*, *FlgE*, *FlgD*, *FliC*, and *FliD*) and biofilm formation (*LapA* and *LapF*). The web tool CRISPR Finder was used for the identification and comparative analysis of CRISPR/Cas systems between genomes [32]. AntiSMASH [33] was used for comparative analysis of secondary metabolite gene clusters. PHASTER server (PHAge Search Tool Enhanced Release) was used for the identification and comparative analysis of prophage among genomes. The Comprehensive Antibiotic Resistance Database (CARD) was used to identify and compare potential antibiotic resistance genes among genomes [34].

2.4. Cell Suspension and Cell-Free Suspension Preparation

The cell suspension was prepared from the bacterial culture of PCL1760 grown overnight in (KB) medium at 28 ± 1 °C. The culture was centrifuged at 4000 rpm for 15 min at 4 °C. The precipitate obtained was then washed with sterile phosphate-buffered saline (PBS) (140 mM NaCl, 5 mM KH_2PO_4, 1 mM $NaHCO_3$, pH 7.4) and resuspended in the same solution to an optical density value of 0.5 at 595 nm. The cell-free suspension was obtained by centrifugation at 10,000 rpm for 10 min at 4 °C of PCL1760 culture grown in King's B (KB) medium at 35 ± 1 °C for 5 days. The supernatant obtained was aseptically filtrated (through a 0.20 µm pore-size membrane filter).

2.5. Antagonistic Activities

The ability of *P. putida* PCL1760 to inhibit the growth of pathogenic bacteria (Table 2) was performed on KB agar medium using the dual culture and disc-diffusion method. For this purpose, 100 µL of an overnight culture of each phytopathogenic bacteria with an optical density (595 nm) value of 0.05 was plated on King's B agar using a plate spreader, and then cell and cell-free suspension of PCL1760 were co-inoculated on the same plate using cotton wool discs (which were amended with 50 µL of the suspension). The plates were then incubated at 28 ± 1 °C for 3 days. The formation of a clear zone around the growing bacteria was considered as a positive antagonistic activity.

Table 2. Pathogenic bacterial strains used in this study for antagonistic activity.

Pathogenic Bacterial Strains	References
Pseudomonas syringae pv. tomato DC3000	Cuppels and Ainsworth [35]
Staphylococcus aureus RN6390	Khusainov et al. [36]
Pseudomonas aeruginosa IR1.5	Egamberdieva et al. [37]

In addition, to validate the functionality of the AMR gene found in the genome of PCL1760, the antibiotic susceptibility test was assayed using the disc-diffusion method. Antibiotics used for this purpose included ampicillin (Ap), Ceftriaxone (Cef), Chloramphenicol (Cm), Ciprofloxacin (Cf), Erythromycin (Em), Kanamycin (Km), Moxifloxacin (Mf), Spectinomycin (Sp), and Tetracycline (Tc). Each antibiotic was used in the range of 0.75–24 µg (0.75 µg, 1.5 µg, 3 µg, 6 µg, 12 µg, and 24 µg). The antibiogram of *P. putida* PCL1760 was then identified as susceptible (S), intermediate (I), and resistant (R) as recommended by the National Committee for Clinical Laboratory Standard Guidelines [38].

3. Results

3.1. The Genome Assembly, Annotation, and Comparison

Contig blasting revealed that PCL1760 is mapped to the assembled GenBank: CP009974.1 and GenBank: CP002290.1 (https://blast.ncbi.nlm.nih.gov/Blast.cgi, accessed on 25 May 2020) with alignment rates of 100% and 99.55%, respectively. Based on the obtained ANIb result, *P. putida* S12 was selected as a reference genome assembly.

The genomic features of *P. putida* PCL1760 are summarized in Table 3. Based on the annotation provided by the Prokaryotic Genome Annotation Pipeline (PGAP), the full genome of *P. putida* PCL1760 contained a single circular chromosome of 6,002,785 bp with 61.80% G + C. The whole genome of PCL1760 harbors 5215 gene-coding sequences covering 96.53% of the genome, as well as 72 tRNAs, 4 ncRNAs, and 88 pseudogenes. Plasmid genome was not predicted in PCL1760. The genomes of strain Pt14, W-6, S12, PCL1751, and WC417 harbor gene-coding sequences that cover 96.96%, 96.65%, 96.95%, 97.15, and 97.22% of their genomes, respectively, in comparison with PCL1760 (Table 3). Pseudogenes were more commonly predicted in *P. putida* S12. The percentage of pseudogenes for PCL1760, Pt14, W-6, S12, PCL1751, and WCS417 calculated in these genomes was 1.63, 1.32, 1.53, 1.64, 1.12, and 1.42%, respectively, in relation to their total genes. All of the selected genomes harbor identical ncRNAs and proximity identical G + C content (Table 3).

Table 3. Comparative genomic features between *P. putida* PCL1760 and related strains.

Features	PCL1760	Pt14	W-6	S12	PCL1751	WCS417
Genome size (bp)	6,002,785	5,841,722	6,190,190	6,382,434	6,143,950	6,169,071
G + C (%)	61.80	60.30	62.70	61.44	60.40	60.30
Genes (total)	5402	5301	5674	5888	5668	5692
CDSs (total)	5303	5210	5571	5805	5575	5615
Genes (coding)	5215	5140	5484	5708	5507	5534
Genes (RNA)	99	91	103	83	93	77
tRNAs	72	68	76	61	70	64
ncRNAs	4	4	5	4	4	4
Pseudo genes (total)	88	70	87	97	68	81
Plasmid	0	0	0	0	0	0
CRISPR-elements	5	11	1	3	2	1
Cas3 elements type I	10	16	16	12	14	14

The comparative analysis of CRISPR/Cas revealed that *P. putida* PCL1760 harbors five CRISPR elements (Tables 3 and S1), as compared with strains Pt14, W-6, S12, PCL1751, and WCS417, in which 11, 1, 3, 2, and 14 CRISPR elements were predicted, respectively (Tables 3 and S2–S6). All compared genomes had a Cas cluster containing different numbers of the same Cas3 Type I elements. Moreover, the Cas cluster found in the whole genome of the strain Pt14 and W-6 contained 16 Cas3 elements type I, whereby the Cas cluster present in the strain of S12, PCL1751, and WCS417 harbors 12, 14, and 14 Cas3 elements type I, respectively (Table 3).

Average nucleotide identity comparison of PCL1760 with the selected strains revealed that PCL1760 is closely related to *P. putida* S12, with an average nucleotide identity of 98.39% (based on BLAST) and 97.5% (based on the average aligned nucleotide). *P. simiae* strains (PCL1751 and WCS417) and *P. fluorescens* strains (W-6 and Pt14) have an average nucleotide similarity (based on BLAST) of less than 90% and 80%, respectively, based on the average aligned nucleotide with *P. putida* strains PCL1760 and S12 (Table 4).

Table 4. Average nucleotide identity comparison of *P. putida* PLC1760 with related strains of *Pseudomonas* genera based on BLAST.

	PCL1760	S12	Pt14	W-6	PCL1751	WCS417
PCL1760	–	**99.30** (*94.29*)	**76.06** (*51.55*)	**75.82** (*52.16*)	**76.26** (*52.29*)	**76.26** (*52.27*)
S12	**99.75** (*94.84*)	–	**76.32** (*51.84*)	**76.03** (*52.22*)	**76.38** (*52.58*)	**76.35** (*52.68*)
Pt14	**76.40** (*50.52*)	**76.45** (*50.53*)	–	**85.65** (*75.31*)	**86.08** (*77.14*)	**86.04** (*77.26*)
W-6	**75.78** (*50.40*)	**75.77** (*50.22*)	**85.44** (*72.36*)	–	**86.57** (*77.32*)	**86.59** (*77.25*)
PCL1751	**76.30** (*50.29*)	**76.32** (*50.11*)	**85.82** (*74.17*)	**86.73** (*76.41*)	–	**99.50** (*95.70*)
WCS417	**76.15** (*49.73*)	**76.12** (*49.60*)	**85.70** (*73.71*)	**86.57** (*76.28*)	**99.41** (*95.25*)	–

N.B. ANI (average nucleotides aligned)—data in italic; ANIb (average nucleotides aligned based on BLAST)—data in bold.

Prophage analysis of PCL1760 using PHASTER revealed three prophages, of which one region is intact, one is incomplete, and one is questionable (Table S7). The intact prophage in the genome regions 3,796,726–387,790 nucleotides (nt) of PCL1760 was predicted to be similar to the most common phage Pseudo YMC11/02/R656 NC 028657, while the questionable prophage found in the genome regions 5,159,654–5,188,739 nt was predicted to be similar to the PHAGE Pseudo JBD44 NC 030929. The incomplete phage in the genome region 735,221–772,596 nt was identified as PHAGE Escher 500465 1 NC 049342.

In comparison with the strain of PCL1760, no intact and questionable prophages were predicted in *P. putida* S12 (Table S8). The presence of these three incomplete phage regions in *P. putida* S12 is similar to the most common phage PHAGE *Escher* 500465 1 NC 049342, PHAGE *Pseudo* JBD44 NC 030929, and PHAGE *Bacill* vB BtS BMBtp14 NC 048640 (Table 5). *P. fluorescens* Pt14, *P. simiae* WCS417, *P. simiae* PCL1751, and *P. fluorescens* W-6 carried four prophages (two intact and two incomplete); two prophages (two intact); four prophages (two intact, one questionable, and one incomplete); and two prophages (intact and incomplete), respectively (Tables S9–S12). Two identical prophages similar to the most common phage PHAGE *Vibrio* VP882 NC 009016 and PHAGE *Pseudo* YMC11/02/R656 NC 028657 were predicted in *P. fluorescens* Pt14, *P. simiae* WCS417, and *P. simiae* PCL1751. The presence of the intact phage PHAGE Pseudo YMC11/02/R656 NC 028657 was also predicted in *P. fluorescens* W-6 (Table 5).

Table 5. Comparison of the prophage predicted in related bacterial strains.

Predicted Prophages	The Presence (+) or Absence (−) in Related Bacterial Strains					
	PCL1760	**S12**	**Pt14**	**W-6**	**PCL1751**	**WCS417**
PHAGE *Escher* 500465 1 NC 049342	+	+	+	+		−
PHAGE *Pseudo* YMC11/02/R656 NC 028657	+	−	+	+	+	+
PHAGE *Pseudo* JBD44 NC 030929	+	+	−	−	−	−
PHAGE *Bacill* vB BtS BMBtp14 NC 048640	−	+	−	−	−	−
PHAGE *Vibrio* VP882 NC 009016	−	−	+	−	+	+
PHAGE *Pseudo* F10 NC 007805	−	−	+	−	−	−
PHAGE *Vibrio* vB VpaM MAR NC 019722	−	−	−	−	+	−
PHAGE *Salmon* SJ46 NC 031129	−	−	−	−	+	−

The comparison of the AMR gene family is summarized in Table 6. As can be seen, the antibiotic resistance ontology (ARO) *adeF* and *Pseudomonas aeruginosa soxR* belong to the AMR gene family resistance-nodulation cell division (RND) antibiotic efflux pump, an ATP binding cassette (ABC) antibiotic efflux pump, and the major facilitator superfamily (MFS) antibiotic efflux pump, which confers resistance to fluoroquinolone antibiotic, tetracycline antibiotic cephalosporin, glycylcycline, penam, rifamycin antibiotic, phenicol antibiotic, disinfecting agents, and antiseptics. Additionally, an ARO term *Acinetobacter baumannii AbaQ* belonging to the major facilitator superfamily (MFS) antibiotic efflux pump, which confers resistance to the fluoroquinolone antibiotic predicted in strains of Pt14, W-6, PCL1751, and WCS417, was absent in *P. putida* PCL1760 and S12.

Table 6. Antimicrobial resistance gene family between *P. putida* PCL1760 and related bacterial strains.

ARO Term	AMR Gene Family	Drug Class	Resistance Mechanism	The Presence (+) or Absence (−) in Related Bacterial Strains					
				PCL1760	**S12**	**Pt14**	**W-6**	**PCL1751**	**WCS417**
adeF	Resistance-nodulation-cell division (RND) antibiotic efflux pump	fluoroquinolone antibiotic, tetracycline antibiotic	antibiotic efflux	+	+	+	+	+	+
*Pseudomo-nas aeruginosa sox*R	ATP-binding cassette (ABC) antibiotic efflux pump, major facilitator superfamily (MFS) antibiotic efflux pump, resistance-nodulation-cell division (RND) antibiotic efflux pump	fluoroquinolone antibiotic, cephalosporin, glycylcycline, penam, tetracycline antibiotic, rifamycin antibiotic, phenicol antibiotic, disinfecting agents and antiseptics	antibiotic target alteration, antibiotic efflux	−	−	+	+	+	+
Acinetobacter baumannii *Aba*Q	major facilitator superfamily (MFS) antibiotic efflux pump	fluoroquinolone antibiotic	antibiotic efflux	−	−	+	+	+	+

The comparison of gene clusters related to the biosynthesis of secondary metabolites using antiSMASH is presented in Table 7. Nine and eight gene clusters were found in the PCL1760 and S12 genomes, respectively, related to the biosynthesis of secondary metabolites (Figure S1A,B). The putative gene clusters in PCL1760 were two cluster types encoding NRPS (non-ribosomal peptide synthetase) with 14 and 19% similarity to the most known pyoverdin biosynthetic gene cluster, one redox-cofactor with 13% similarity to lankacidin C, two RIPPs-like (other unspecified ribosomally synthesized and post-translationally modified peptide product (RiPP) cluster) type, one T1PKS (type I polyketide synthetase) with 27% similarity to the most known O-antigen biosynthetic gene cluster, one RRE-containing

(RRE-element containing cluster), one NAGGN (N-acetylglutaminylglutamine amide), and a ranphipeptides type cluster (Cys-rich peptides). The ranphipeptides type cluster had 7% similarity to the most known cluster for the synthesis of pyoverdin. The ranphipeptide-type gene cluster was absent from the genome of S12. Furthermore, four gene cluster types (NAGGN, RRE-containing, and two RIPPs-like) related to the biosynthesis of secondary metabolites in PCL1760 and S12 did not correspond to the most known cluster.

Table 7. The comparison of gene clusters related to the biosynthesis of secondary metabolites between *P. putida* PCL1760 and related bacterial strains.

Secondary Metabolites Related to the Most Known Biosynthesis Cluster Genes	The Presence (+) or Absence (−) in Related Bacterial Strains					
	PCL1760	**S12**	**Pt14**	**W-6**	**PCL1751**	**WCS417**
O-antigen	+	+	+	+	+	+
lankacidin C	+	+	+	+	+	+
pyoverdin	+	+	+	+	+	+
fengycin	−	−	+	+	+	+
APE-vf	−	−	+	+	+	+
Coelibactin	−	−	−	+	+	+
L-2-amin0-4-methoxy-trans-3-butenioc acid	−	−	−	+	−	+
Pseudomonine	−	−	+	−	−	−
Ambactin	−	−	+	−	−	−

As compared with *P. putida* strains PCL1760 and S12, twelve gene cluster types were found to be associated with the biosynthesis of secondary metabolites in W-6, Pt14, PCL1751, and WCS417 (Figure S1C–F). The presence of siderophores, arylpolyene, hserlactone, terpene, and betalactone gene cluster types in these genomes was predicted. Each genome harbored three cluster types NRPS (non-ribosomal peptide synthetase) with less than 19% similarity to the most known pyoverdin biosynthetic gene cluster in comparison with PCL1760 and S12. The cluster type betalactone was predicted as a fengycin biosynthetic gene cluster with 13% similarity in all analyzed strains, except the two *P. putida* strains, PCL1760 and S12 (Table 7). The gene cluster type arylpolyene, absent in *P. putida* PCL1760 and S12, but present in *P. fluorescens* W-6, Pt14, *P. simiae* PCL1751, and WCS417, was found to be less than 50% similar to the APE-vf biosynthesis gene cluster. The cluster responsible for the synthesis of pseudomonine (with 100% similarity) with siderophoric activity and ambactin (with 25% similarity) was only predicted in *P. fluorescens* Pt14.

Coelibactin biosynthesis gene cluster was only predicted in *P. simiae* WCS417, PCL1751, and *P. fluorescens* W-6. The NRPS-like cluster type with 40% similarity to the most known L-2-amino-4-methoxytrans-3-butenioc acid biosynthesis cluster was only predicted in strains of *P. fluorescens*. Five types of clusters (terpene, RIPP-like, NAGGN, and hserlactone) present in *P. simiae WCS*417, *P. fluorescens* W-6, *P. fluorescens* Pt14, and *P. simiae* PCL1751 have no identified biosynthesis cluster (Figure S1).

The pangenome analysis using Roary identified a total of 14,548 genes. The core genome comprised 467 (3.22%) genes present in all selected bacterial strains. The accessory genome included 14,081 (96.78%) shell genes (15% $\leq$ strains < 95%). No cloud genes (0% $\leq$ strains < 15%) and soft-core gene (95% $\leq$ strains < 99%) were predicted among the compared bacterial strains (Figure 1).

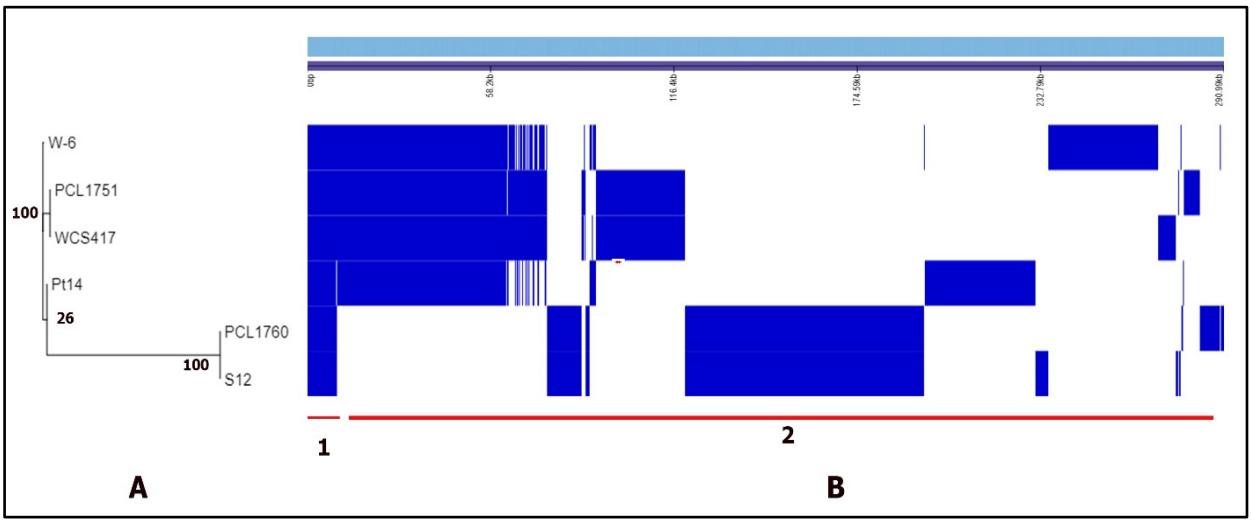

Figure 1. Pangenome analysis of *P. putida* PCL1760 with related strains using Roary. The whole-genome alignment of the selected strains was clustered based on the presence (in blue color) and absence (in white color) of genes in each strain, which was visualized with Phandango [39]. A phylogeny (**A**) was generated based on genes shared by the strain of PCL1760 with Pt14, W-6, S12, PCL1751, and WCS417. Roary representation (**B**) of core genome (1) and accessory genome (2) among selected bacterial strains.

The analysis of orthologous gene clusters using OrthoVenn2 revealed that the species form 6905 clusters, 3788 (54.86%) orthologous clusters (at least contain two species), and 3117 single-copy gene clusters. PCL1760, Pt24, W-6, S12, PCL1751, and WCS417 harbored 4920, 4702, 4817, 4890, 5347, and 5375 clusters, respectively, and 278, 469, 613, 161, 172, and 192 proteins, respectively, that are unique to the strains (Table 8).

Table 8. Comparison of the number of proteins, orthologous clusters, and singletons predicted in the strain of PCL1760 and related bacterial strains assembly using OrthoVenn2.

Species	Cluster	Singletons
P. putida PCL1760	4920	278
P. simiae PCL1751	4702	469
P. fluorescens Pt14	4817	613
P. simiae WCS417	4890	161
P. putida S12	5345	172
P. fluorescens W-6	5375	192

The genome of *P. putida* PCL1760 shares a core gene of 3208 orthologous gene clusters with genomes of *P. putida* S12, *P. simiae*, and *P. fluorescens* strains (Figure 2).

Strains PCL1760, Pt 24, W-6, S12, PCL1751, and WCS417 had 4, 10, 17, 5, 3, and 2 clusters of genes, respectively, which are not included in orthologous clusters (Figure 2B). These unique gene clusters found in PCL1760 were related to the oxidoreductase activity response, DNA-binding transcription factor activity, and the putrescine catabolic process (Figure S2). Those found in Pt24 were related to phosphorelay sensor kinase activity and transposition, as well as DNA-mediated signaling (Figure S3). The gene clusters found in the strain of W-6 were associated with the antigen biosynthetic process, hydrolase activity, protein secretion by the type II secretion system, nitrogen compound metabolic process, ion transport, carbohydrate metabolic process, and transmembrane transport (Figure S4).

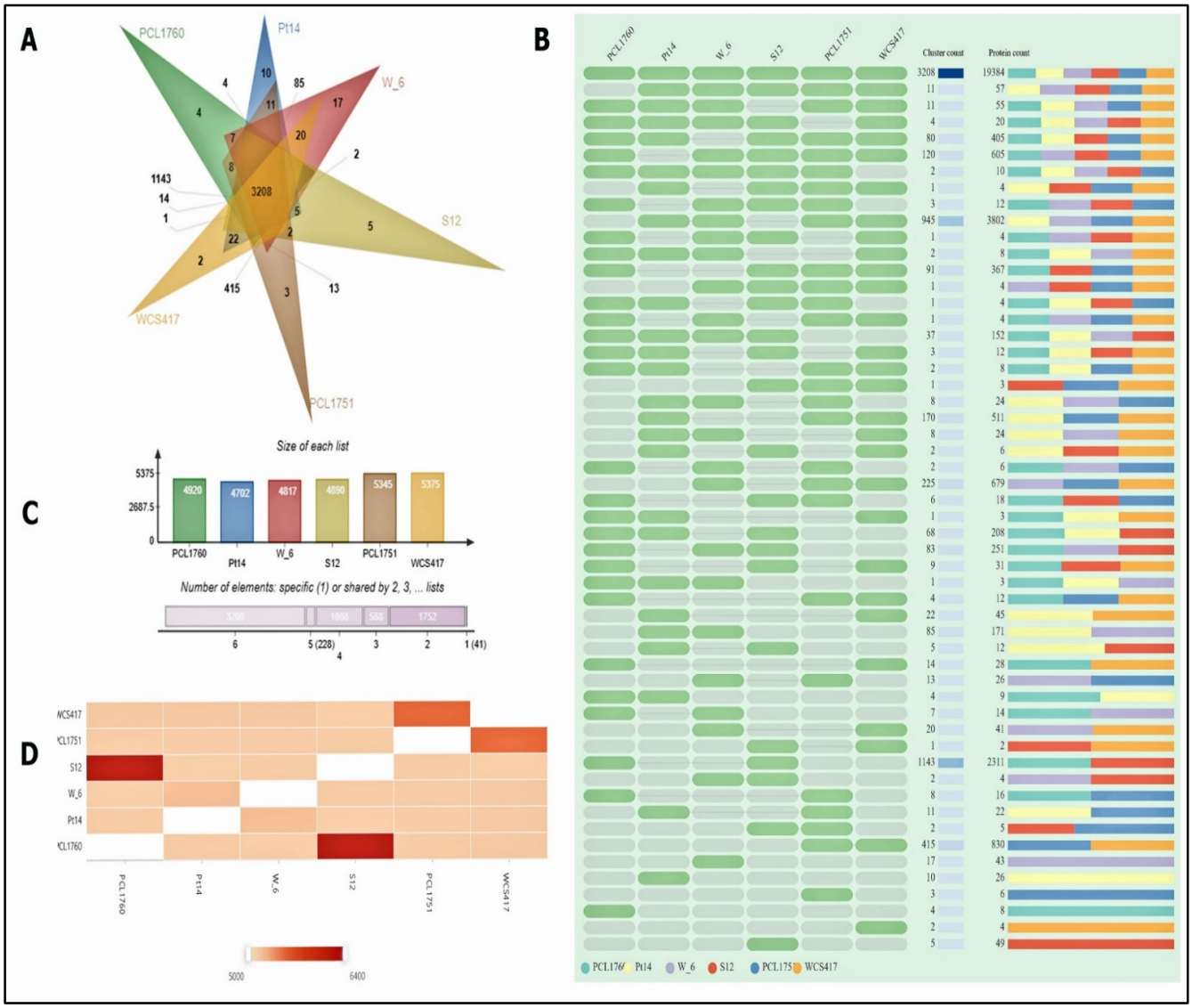

Figure 2. The analysis of orthologous gene clusters using OrthoVenn2. (**A**) Venn diagram presentation of orthologous clusters distributed among *P. putida* PCL1760 and related species. (**B**) Summary of protein harbored by each species. (**C**) Orthologous gene clusters' distribution and proteins counted among *P. putida* PCL1760 and related strains of *Pseudomonas* genus. (**D**) Similarity matrix for paired genome comparisons showing a heat map between genomes.

In the strain of S12, these five clusters are responsible for transposition (putative transposase y4uL), ATP binding (putative insertion sequence ATP-binding protein y4pL), and response to chromate stress (Figure S5). The clusters found in PCL1751 are related to the DNA restriction-modification system (Figure S6). In the strain of WCS417, no function was associated with the two clusters (Figure S7).

The strain of PCL1760 and S12 shared 1143 orthologous gene clusters (Figure 1B). Among them are orthologous clusters involved in the butanediol metabolic process (Acetolactate synthase, catabolic), bacteriocin immunity (Colicin-E7 immunity protein), pilus assembly, cell adhesion (Fimbrial protein), capsule polysaccharide biosynthetic process (Gamma-glutamyl-CDP-amidate hydrolase), cellular response to nitric oxide, riboflavin biosynthetic process, purine nucleobase metabolic process, biotin biosynthetic process, biotin biosynthetic process, metal ion binding, antibiotic biosynthetic process (Mycosubtilin synthase subunit C), aromatic compound catabolic process (2,4-dinitrotoluene dioxygenase

system, ferredoxin component), creatinase activity, protein secretion by the type II secretion system (type II secretion system protein I), and others (Figure S8).

The strains PCL1760 and S12 each share 11 orthologous clusters with Pt14, W-6, PCL1751, and WCS417 (Figure 2B). Among orthologous clusters shared by PCL1760 with Pt24, W-6, PCL1751, and WCS417, clusters responsible for the viral protein involved in tail assembly, virion attachment to host cell, glycine betaine transport, signal transduction, and others were present (Figure S9). In addition, some of the clusters shared by S12 with other strains, with the exception of PCL1760, include clusters responsible for transferase activity (transferring glycosyl groups), aromatic compound catabolic process (Figures S10 and S11), galactonate catabolic process, phosphorelay sensor kinase activities, response to cadmium ion, inositol catabolic process (Figure S12), basic amino acid transport, and other clusters.

Nine hundred and forty-five orthologous gene clusters are shared by Pt24, W-6, PCL1751, and WCS417 strains. Among the clusters found are those responsible for purine nucleoside transmembrane transporter activity, regulation of carbohydrate catabolic process, response to antibiotics, 3-phytase activity, fatty acid beta-oxidation, macromolecule deacylation, and other clusters (Figure S13). The BlastN search method revealed the presence of genes involved in the functional motility of the strains, flagella (*FlgK*, *FlgL*, *FlgE*, *FlgD*, *FliC*, and *FliD*), and biofilm formation (*LapA* and *LapF*).

3.2. Antagonistic Activity

Antagonistic activity tested on KB medium revealed the ability of cell suspension of *P. putida* PCL1760 to inhibit directly the growth of pathogenic bacteria *P. syringae* DC3000 (Figure 3B), but not *S. aureus* RN6390 and *P. aeruginosa* IR1.5 (Figure 3A,C), as *Bacillus velezensis* KS04AU did. This can be observed by the appearance of a yellow-greenish zone of inhibition around the colony of PCL1760 (Figure 3B).

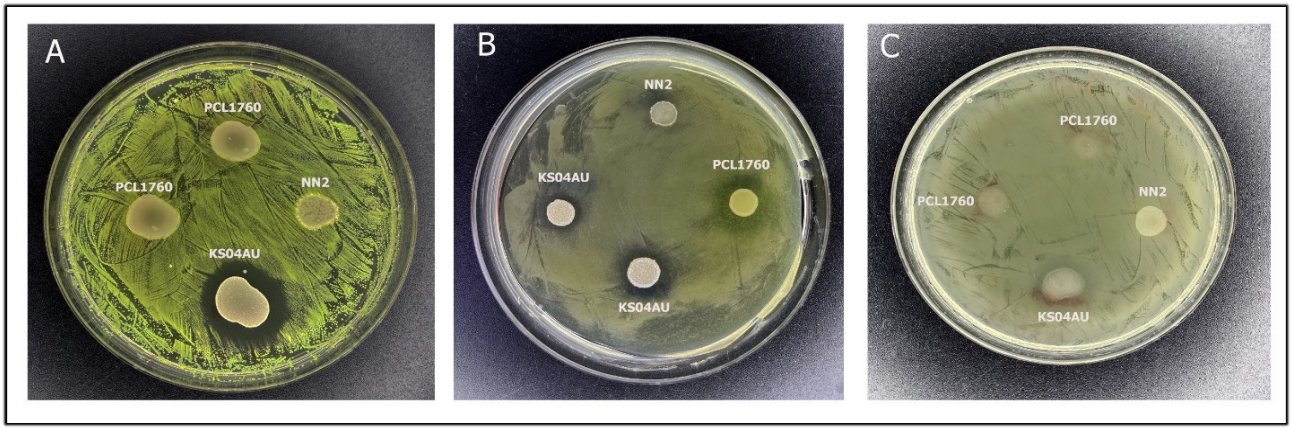

Figure 3. Antagonistic activity of *P. putida* PCL1760 against *S. aureus* RN6390 (**A**), *P. syringae* DC3000 (**B**), and *P. aeruginosa* IR1.5 (**C**). *Bacillus velezensis* KS04AU and *Bacillus aryabhattai* NN2 were used as positive and negative controls, respectively.

However, a different result was obtained with the PCL1760 cell-free supernatant (Figure 4). No antagonistic activity against pathogenic bacteria tested was observed.

The antibiogram result of PCL1760 against nine antibiotics is represented in Table 9. The antibiotic susceptibility test of the nine antibiotics showed PCL1760 to be resistant to erythromycin, ampicillin, chloramphenicol, and spectinomycin, as well as an intermediate resistance to tetracycline when 24 µg of the antibiotic was applied. High susceptibility of PCL1760 against moxifloxacin was observed in all ranges of antibiotics per filter disc used in the experiment (Figure S16). A partial or intermediate susceptibility was observed against ciprofloxacin, kanamycin (≤3 µg), and Ceftriaxone (≤1.5 µg).

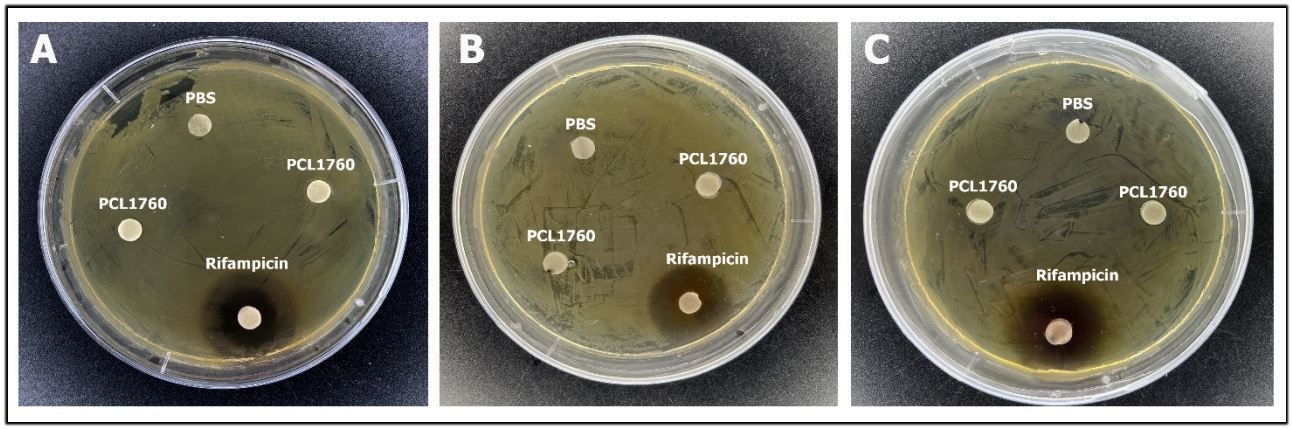

Figure 4. Antagonistic activity of cell-free supernatant obtained from *P. putida* PCL1760 against *S. aureus* RN6390 (**A**), *P. syringae* DC3000 (**B**), and *P. aeruginosa* IR1.5 (**C**). Rifampicin and sterile PBS were used as positive and negative controls, respectively.

Table 9. Antibiotic susceptibility test of *Pseudomonas putida* strain PCL1760.

Antibiotics	Masses of Antibiotics and Susceptibility of *P. putida* PCL1760					
	0.75 µg	1.5 µg	3 µg	6 µg	12 µg	24 µg
Erythromycin	R	R	R	R	R	R
Ciprofloxacin	R	I	I	S	S	S
Moxifloxacin	S	S	S	S	S	S
Ampicillin	R	R	R	R	R	R
Chloramphenicol	R	R	R	R	R	R
Kanamycin	I	I	I	S	S	S
Ceftriaxone	I	I	S	S	S	S
Spectinomycin	R	R	R	R	R	R
Tetracycline	R	R	R	R	R	I

Legend: (S)–Susceptible, (I)– intermediate and (R)–resistant.

4. Discussion

The biocontrol ability of *P. putida* PCL1760 against tomato foot and root rot disease (*Forl* ZUM2407) through CNN and the absence of hydrolytic enzyme activity has been well documented [4]. As there is a shift to engineering bacteria cells rather for the catabolism of complex substrates, there is a tendency to search for new model systems. To investigate the absence of genes responsible for antibiosis and how suitable our strain is to be genetically manipulated for biotechnological applications, there was the need to annotate the full genome sequence of PCL1760 and confirm the antagonistic activity of the strain.

The antagonistic activity against the bacterial phytopathogen *P. syringae* also brought our attention to study the sequence of the full genome of PCL1760 to find the active compound inhibiting the pathogen [40]. Ye et al. [16] studied the antimicrobial activity of *P. putida* strain W15Oct28 on the phytopathogen *P. syringae* and other bacterial pathogens based on putisolvin biosynthesis. The authors observed antagonistic activity of *P. putida* on *Staphylococcus aureus*, *P. aeruginosa*, and *P. syringae*. In our case, *P. putida* PCL1760 was able to inhibit only *P. syringae*, which was profound on minimal media (Figure S15A), than KB agar (Figure S15B) suggesting the occurrence of inhibition being a siderophoric activity. This is observed by the fewer cell or halo zones with yellow-greenish fluorescence around the colonies of PCL1760. In addition, secondary metabolites of cell-free supernatant did not inhibit the pathogen, suggesting either effector genes are released by *P. syringae*

to activate the production of siderophores as competition for nutrients, triggering the inhibition effect in dual culture experiments (Figure 4). The analysis of 16 rhizobacteria strains from the ginseng plant showed a weak antagonistic effect of siderophore of all *P. putida* strains in comparison with the strain *P. putida* KNUK9, being eminent in inhibiting the fungus *Aspergillus niger* [41]. The above discussion suggests that not all *P. putida* strains possess the antibiosis mechanism, and confirms the mechanism of CNN as being the sole biocontrol mechanism of PCL1760 against phytopathogens and its application in the greenhouse [4,15].

The advantages of *P. putida* strains in industrial biotechnology have been well reported by Weimer et al. [42]. In this mini-review article, the authors present beneficial applications of *P. putida* strains in several genome-scale metabolic models, as transcriptomic and proteomic models, in the production of polyhydroxyalkanoates (PHA), as a multi-omics integration agent and its use in bioremediation. The two most popular strains adapted in industrial and genetic biotechnological applications are *P. putida* KT2440 and *P. putida* S12, domesticated for their easy genetic manipulations and inducible promoter systems for high expression of proteins [42,43]. Recent work on these strains includes the efficient catalytic transformation of D-fructose to 2,5-Bis(hydroxymethyl)furan or improved bioproduction of PHA from styrene vapors by S12 [44,45] and the improved production of muconate from p-coumarate by KT2440 through the conversion of lignin-related aromatic compounds [46]. The authors explain how *PobA*, the native *P. putida* flavoprotein oxygenases, was replaced with *PraI*, a flavoprotein oxygenases of *Paenibacillus* sp. JJ-1b turned to alleviate the inhibition caused by the accumulation of 4-hydroxybenzoate, thereby increasing muconic synthesis. As *P. putida* has well been adapted for the above purposes, the variation in the genetic compositions in different strains helps in the search for new model strains, with a less robust genome to manipulate for its use in the biodegradation of different complex substrates. For this purpose, we decided to analyze the full genome of the well-published *P. putida* strain and confirm its applicability in comparison with the known model S12 as a novel model for genetic biotechnological applications.

One important characteristic of *P. putida* PCL1760 is the adaptative property to some xenobiotics, rendering it a resistant strain to be used in biotechnological applications in terms of viability to resist some antibiotics (Table 6). Although all of the different *Pseudomonas* species compared had more antibiotic-resistant genes present in their genome, the two *P. putida* strains (PCL1760 and S12) had antibiotic efflux pump *adeF* genes able to prevent the actions of DNA synthesis inhibitors, fluoroquinolone, and tetracycline antibiotics [47,48]. The antibiotic susceptibility test of fluoroquinolone and tetracycline antibiotics showed intermediate resistance to ciprofloxacin ($\leq$3 µg), but not moxifloxacin. Tetracycline resistance was higher in comparison with the fluoroquinolone antibiotics, as observed in *P. putida* by Igbinosa et al. [49]. Interestingly, antibiogram tests of the nine antibiotics against PCL1760 also revealed resistance to macrolide, aminopenicillin, amphenicol, and aminocyclitol class of antibiotics, although the CARD server did not predict these genes. AntiSMASH results of the PCL1760 genome showed no secondary metabolite operon responsible for volatile antifungal compounds, which are not needed in terms of genetic reconstructions. Pyoverdin (NRP) siderophore was present in all of the compared strains, but with a low percentage similarity, 7–19% (Figure S1). In comparison with S12, both had secondary metabolites, which included lankacidin C (NRP + Polyketide) and O-antigen (Saccharide) and pyoverdin showing the only mechanism for their inhibition by the uptake of essential trace metal ions for microbial growth. Another interesting piece of information is the absence of core genes (*AmbA*, *AmbB*, *AmbC*, *AmbD*, *AmbE*) for the synthesis of L-2-amino-4-methoxy-trans-3-butenoic acid (AMB)—a toxin against prokaryotes and eukaryotes, in the clusters of *P. simiae* PCL1751, *P. simiae* WCS417, and *P. fluorescens* W-6 [50]. This suggests the possibility of the strains losing these 'luxury' genes, thereby controlling plant diseases by CNN, as confirmed in *P. putida* PCL1760.

Gene clusters on the genomic server, Orthovenn2, showed the presence of genes responsible for cadmium ions and mandelamide amidase or hydrolase (*Pseudomonas* man-

delamide hydrolase) activity in all compared strains except for PCL1760 and W-6. As observed in these *Pseudomonas* strains analyzed, a study was reported on a different *P. putida* strain ATCC 12633 that harbors an operon responsible for the catabolic activity of mandelate that can be a sole carbon source for cell growth [51]. Another interesting finding is the presence of gene clusters responsible for aromatic compounds including inositol catabolic processes in all the tested strains. In contrast to S12, only one cluster gene was found in PCL1760 that was responsible for aromatic compounds catabolism and identical to S12, whilre S12 harbors the gene cluster also responsible for mandelamide amidase activity (Figure S14). The absence of these gene clusters shows *P. putida* PCL1760 as a suitable biotransformation host organism for easy cloning of operons responsible for the biocatalysts of complex aromatic compounds without the interference of other 'autochthonous' operons [52].

An important genetic characteristic in the genome for bacteria immunity against bacteriophages is the presence of CRISPR/Cas and Prophage genes, which can also be manipulated by anti-CRISPR genes of some phages to bypass the immune system of bacteria [53,54]. In this case, the greater the number of CRISPR genes present in the genome, the wider the resistance to other phages or the lower the chance of the strain encountering anti-CRISPR genes to manipulate their defense system. From the results obtained, in comparison with the two *P. putida* strains (KT2440 and S12) as robust laboratory 'work horses' [43], PCL1760 might have an advantage over S12 (5 to 3 CRISPR genes, respectively). Prophages exist in the genome of bacteria after lysogenic infection by bacteriophages as a 'moron' gene (enhancing the immunity of the host), as phage-encoding toxins (to increase virulence in pathogens), or as cryptic prophages (to help bacteria adapt to adverse conditions) [55–57]. In our study, PCL1760 and S12 had the same number of Prophages, but PCL1760 had an intact unique Pseudo YMCII in comparison with the incomplete Bacilli-v8-BIS-BMBtp14 of S12. Although prophages have been proposed to have a link with CRISPR spacers targeting protospacers or STS (self-targeting spacers) to promote auto-immunity, there is still an innate immunity in the acquisition of prophages [58,59]. Thus, the full genomic comparison of *P. putida* PCL1760 to the closely related strain S12 and the other species of *Pseudomonas* analyzed in this work confirms the CNN mechanism of PCL1760 and its genomic amenability for genetic engineering.

5. Conclusions

In summary, the full genome analysis helped to confirm the CNN mechanism of *P. putida* strain PCL1760 as a sole mechanism for protecting plants against microbial pathogens. This was based on the low percentage similarity of the predicted secondary metabolites biosynthesis gene and the absence of cluster genes responsible for antibiosis. The inhibition effect on *P. syringae* might be due to siderophores (pyoverdin) in the gene clusters of PCL1760, which chelate essential trace metal ions, which can be also considered as a CNN mechanism. The genomic comparison to the known model strain *P. putida* S12 thus suggests PCL1760 as a competitive strain in terms of immunity (CRISPR/Cas and Prophages), antibiotic resistance, and its flexibility as a cell factory for genetic manipulations or biosynthesis of desirable organic compounds. The strain has a high prospect not only in agriculture (plant protection and plant growth promoting), but also in biotechnology as a genetic model strain.

Supplementary Materials: The following supporting information can be downloaded at https://www.mdpi.com/article/10.3390/applmicrobiol2040057/s1. Table S1: CRISPR/CAS elements present in *P. putida* PCL1760 using CRISPR Finder; Table S2: CRISPR/CAS elements present in *P. putida* S12 using CRISPR Finder; Table S3: CRISPR/CAS elements present in *P. fluorescens* Pt14 using CRISPR Finder; Table S4: CRISPR/CAS elements present in *P. fluorescens* W-6 using CRISPR Finder; Table S5. CRISPR/CAS elements present in *P. simiae* PCL1751 using CRISPR Finder; Table S6: CRISPR/CAS elements present in *P. simiae* WCS417 using CRISPR Finder; Figure S1: Analysis of secondary metabolites biosynthesis of *P. putida* PCL1760 (A), *P. putida* S12 (B), *P. simiae* PCL1751 (C), *P. fluorescens* Pt14 (D), *P. simiae* WCS417(E), and *P. fluorescens* W-6 (F) using antiSMASH; Table S7: Prophages

predicted in *P. putida* PCL1760 using PHASTER; Table S8. Prophages predicted in *P. putida* S12 using PHASTER; Table S9: Prophages predicted in *P. fluorescens* Pt14 using PHASTER; Table S10: Prophages predicted in *P. simiae* WCS417 using PHASTER; Table S11: Prophages predicted in *P. simiae* PCL1751 using PHASTER; Table S12: Prophages predicted in *P. fluorescens* W-6 using PHASTER; Figure S2: Clusters present in the strain of *P. putida* PCL1760 that are not included in any orthologous clusters with other strains; Figure S3: The unique clusters present in the strain of *P. fluorescens* Pt14 that are not included in any orthologous clusters with other strains; Figure S4: The unique clusters present in the strain of *P. fluorescens* W-6 that are not included in any orthologous clusters with other strains; Figure S5: The unique clusters present in the strain of *P. putida* S12 that are not included in any orthologous clusters with other strains; Figure S6: The unique clusters present in the strain of *P. simae* PCL1751 that are not included in any orthologous clusters with other strains; Figure S7: The unique clusters present in the strain of *P. simae* WCS417 that are not included in any orthologous clusters with other strains; Figure S8: Orthologous gene clusters shared by PCL160 with the strain of S12; Figure S9: Clusters shared among strains of PCL1760, Pt14, W-6, PCL1751, and WCS417; Figure S10: Clusters shared among strains of Pt14, W-6, S12, PCL1751, and WCS417; Figure S11: Cluster GO:0019439; P:aromatic compound catabolic process; IEA:UniProtKB-KW shared by the strain of PCL1760 with Pt14, W-6, S12, PCL1751, and WCS417. Layout of the cluster (A); multiple sequence alignment (B), phylogenetic tree (C); Figure S12: Cluster GO:0019310; P:inositol catabolic process; IEA:UniProtKB-UniRule shared by the strain of PCL1760 with Pt14, W-6, S12, PCL1751, and WCS417. Layout of the cluster (A), multiple sequence alignment (B), and phylogenetic tree (C); Figure S13: Clusters shared among strains of Pt14, W-6, PCL1751, and WCS417 that are not included in any orthologous clusters with other strains; Figure S14: Cluster GO:0050537, F:mandelamide amidase activity; IDA:UniProtKB shared by the strain of Pt14, S12, PCL1751, and WCS417; Figure S15: Antagonistic activity of *P. putida* PCL1760 against *P. syringae* DC300 on M9 minimal (A) and LB (B) agar plates. *Bacillus velezensis* KS04AU and *Bacillus aryabhattai* NN2 were used as positive controls, respectively; Figure S16: The antibiotic susceptibility test of *P. putida* PCL1760 using the disk diffusion method performed on Multer–Hinter agar.

Author Contributions: Conceptualization, S.Z.V. and D.M.A.; methodology, R.G.C.D., E.S.K. and A.K.M.; software, R.G.C.D.; validation, D.M.A. and S.Z.V.; formal analysis, R.G.C.D. and D.M.A.; investigation, D.M.A., R.G.C.D., A.K.M., and E.S.K.; data curation, D.M.A.; writing—original draft preparation, D.M.A. and R.G.C.D.; writing—review and editing, S.Z.V., D.M.A. and R.G.C.D.; supervision, D.M.A. and S.Z.V.; project administration, S.Z.V. All authors have read and agreed to the published version of the manuscript.

Funding: The study was conducted with financial support provided by the Ministry of Education and Science of the Russian Federation, Grant No. 075-15-2022-254 17.06.2022 (13.2251.21.0126).

Institutional Review Board Statement: Not applicable.

Informed Consent Statement: Not applicable.

Data Availability Statement: Not applicable.

Conflicts of Interest: The authors declare that they have no known competing financial interests or personal relationships that could have appeared to influence the work reported in this paper.

References

1. O'Brien, P.A. Biological control of plant diseases. *Australas. Plant Pathol.* **2017**, *46*, 293–304. [CrossRef]
2. Punja, Z.K.; Utkhede, R.S. Using fungi and yeasts to manage vegetable crop diseases. *Trends Biotechnol.* **2003**, *21*, 400–407. [CrossRef]
3. Khabbaz, S.E.; Zhang, L.; Cáceres, L.A.; Sumarah, M.; Wang, A.; Abbasi, P.A. Characterisation of antagonistic Bacillus and Pseudomonas strains for biocontrol potential and suppression of damping-off and root rot diseases. *Ann. Appl. Biol.* **2015**, *166*, 456–471. [CrossRef]
4. Validov, S.Z.; Kamilova, F.; Lugtenberg, B.J. Pseudomonas putida strain PCL1760 controls tomato foot and root rot in stonewool under industrial conditions in a certified greenhouse. *Biol. Control.* **2009**, *48*, 6–11. [CrossRef]
5. Bernal, P.; Allsopp, L.P.; Filloux, A.; Llamas, M.A. The Pseudomonas putida T6SS is a plant warden against phytopathogens. *ISME J.* **2017**, *11*, 97–2987. [CrossRef]

6. Agisha, V.N.; Kumar, A.; Eapen, S.J.; Sheoran, N.; Suseelabhai, R. Broad-spectrum antimicrobial activity of volatile organic compounds from endophytic Pseudomonas putida BP25 against diverse plant pathogens. *Biocontrol. Sci. Technol.* **2019**, *29*, 1069–1089. [CrossRef]
7. Patten, C.L.; Glick, B.R. Role of Pseudomonas putida indoleacetic acid in development of the host plant root system. *Appl. Environ. Microbiol.* **2002**, *68*, 3795–3801. [CrossRef]
8. Rawat, P.; Das, S.; Shankhdhar, D.; Shankhdhar, S.C. Phosphate-solubilizing microorganisms: Mechanism and their role in phosphate solubilization and uptake. *J. Plant Nutr. Soil Sci.* **2021**, *21*, 49–68. [CrossRef]
9. Shabayev, V.P. Effect of the introduction of the nitrogen-fixing bacteria Pseudomonas putida 23 on the nitrogen balance in soil. *Eurasian Soil Sci.* **2010**, *43*, 436–441. [CrossRef]
10. Poblete-Castro, I.; Becker, J.; Dohnt, K.; Dos Santos, V.M.; Wittmann, C. Industrial biotechnology of Pseudomonas putida and related species. *Appl. Microbiol. Biotechnol.* **2012**, *93*, 2279–2290. [CrossRef]
11. Schmid, A.; Dordick, J.S.; Hauer, B.; Kiener, A.; Wubbolts, M.; Witholt, B. Industrial biocatalysis today and tomorrow. *Nature* **2001**, *409*, 258–268. [CrossRef] [PubMed]
12. Santos, A.; Mendes, S.; Brissos, V.; Martins, L.O. New dye-decolorizing peroxidases from Bacillus subtilis and Pseudomonas putida MET94: Towards biotechnological applications. *Appl. Microbiol. Biotechnol.* **2014**, *98*, 2053–2065. [CrossRef] [PubMed]
13. Mardani, G.; Ahankoub, M.; Alikhani Faradonbeh, M.; Raeisi Shahraki, H.; Fadaei, A. Biodegradation of ceftriaxone in soil using dioxygenase-producing genetically engineered Pseudomonas putida. *Bioremediat. J.* **2022**, *26*, 1–12. [CrossRef]
14. Amiri, N.A.; Amiri, F.A.; Faravardeh, L.; Eslami, A.; Ghasemi, A.; Rafiee, M. Enhancement of MBBR reactor efficiency using effective microorganism for treatment of wastewater containing diazinon by engineered Pseudomonas putida KT2440 with manganese peroxidase 2 gene. *J. Environ. Manag.* **2022**, *316*, 115293. [CrossRef]
15. Validov, S.Z.; Kamilova, F.; Qi, S.; Stephan, D.; Wang, J.J.; Makarova, N.; Lugtenberg, B.J. Selection of bacteria able to control Fusarium oxysporum f. sp. radicis-lycopersici in stonewool substrate. *J. Appl. Microbiol.* **2007**, *102*, 461–471. [CrossRef]
16. Ye, L.; Hildebrand, F.; Dingemans, J.; Ballet, S.; Laus, G.; Matthijs, S.; Berendsen, R.; Cornelis, P. Draft genome sequence analysis of a Pseudomonas putida W15Oct28 strain with antagonistic activity to Gram-positive and Pseudomonas sp. pathogens. *PLoS ONE* **2014**, *9*, e110038. [CrossRef]
17. Kamilova, F.; Validov, S.; Azarova, T.; Mulders, I.; Lugtenberg, B.j. Enrichment for enhanced competitive plant root tip colonizers selects for a new class of biocontrol bacteria. *Appl. Environ. Microbiol.* **2005**, *7*, 1809–1817. [CrossRef]
18. Rani, P.; Mahato, N.K.; Sharma, A.; Rao, D.L.N.; Kamra, K.; Lal, R. Genome mining and predictive functional profiling of acidophilic rhizobacterium Pseudomonas fluorescens Pt14. *Indian J. Microbiol.* **2017**, *57*, 155–161. [CrossRef]
19. Pieterse, C.M.; Berendsen, R.L.; de Jonge, R.; Stringlis, I.A.; Van Dijken, A.J.; Van Pelt, J.A.; Van Wees, S.C.M.; Yu, K.; Zamioudis, C.; Bakker, H.M. Pseudomonas simiae WCS417: Star track of a model beneficial rhizobacterium. *Plant Soil* **2021**, *461*, 245–263. [CrossRef]
20. Hartmans, S.; Van der Werf, M.J.; De Bont, J.A. Bacterial degradation of styrene involving a novel flavin adenine dinucleotide-dependent styrene monooxygenase. *Appl. Environ. Microbiol.* **1990**, *56*, 1347–1351. [CrossRef]
21. Xiang, Y.; Wang, S.; Li, J.; Wei, Y.; Zhang, Q.; Lin, L.; Ji, X. Isolation and characterization of two lytic cold-active bacteriophages infecting Pseudomonas fluorescens from the Napahai plateau wetland. *Can. J. Microbiol.* **2018**, *64*, 183–190. [CrossRef] [PubMed]
22. Brown, J.; Pirrung, M.; McCue, L.A. FQC Dashboard: Integrates FastQC results into a web-based, interactive, and extensible FASTQ quality control tool. *Bioinformatics* **2017**, *33*, 3137–3139. [CrossRef] [PubMed]
23. Bolger, A.M.; Lohse, M.; Usadel, B. Trimmomatic: A flexible trimmer for Illumina sequence data. *Bioinformatics* **2014**, *30*, 2114–2120. [CrossRef]
24. Wick, R.R.; Judd, L.M.; Gorrie, C.L.; Holt, K.E. Unicycler: Resolving bacterial genome assemblies from short and long sequencing reads. *PLoS Comput. Biol.* **2017**, *13*, e100559. [CrossRef]
25. Darling, A.C.; Mau, B.; Blattner, F.R.; Perna, N.T. Mauve: Multiple alignment of conserved genomic sequence with rearrangements. *Genome Res.* **2004**, *14*, 1394–1403. [CrossRef]
26. Gurevich, A.; Saveliev, V.; Vyahhi, N.; Tesler, G. QUAST: Quality assessment tool for genome assemblies. *Bioinformatics* **2013**, *29*, 1072–1075. [CrossRef] [PubMed]
27. Chu, C.; Li, X.; Wu, Y. GAPPadder: A sensitive approach for closing gaps on draft genomes with short sequence reads. *BMC Genom.* **2019**, *20*, 426. [CrossRef] [PubMed]
28. Tatusova, T.; DiCuccio, M.; Badretdin, A.; Chetvernin, V.; Nawrocki, E.P.; Zaslavsky, L.; Lomsadze, A.; Pruitt, K.D.; Borodovsky, M.; Ostell, J. NCBI prokaryotic genome annotation pipeline. *Nucleic Acids Res.* **2016**, *44*, 6614–6624. [CrossRef]
29. Seemann, T. Prokka: Rapid prokaryotic genome annotation. *Bioinformatics* **2014**, *30*, 2068–2069. [CrossRef]
30. Page, A.J.; Cummins, C.A.; Hunt, M.; Wong, V.K.; Reuter, S.; Holden, M.T.; Parkhill, J. Roary: Rapid large-scale prokaryote pan-genome analysis. *Bioinformatics* **2015**, *31*, 3691–3693. [CrossRef]
31. Xu, L.; Dong, Z.; Fang, L.; Luo, Y.; Wei, Z.; Guo, H.; Zhang, G.; Gu, Q.Y.; Coleman-Derr, D.; Xia, Q.; et al. OrthoVenn2: A Web Server for Whole-Genome Comparison and Annotation of Orthologous Clusters Across Multiple Species. *Nucleic Acids Res.* **2019**, *47*, W52–W58. [CrossRef] [PubMed]
32. Grissa, I.; Vergnaud, G.; Pourcel, C. The CRISPRdb database and tools to display CRISPRs and to generate dictionaries of spacers and repeats. *BMC Bioinform.* **2007**, *8*, 172. [CrossRef] [PubMed]

33. Weber, T.; Blin, K.; Duddela, S.; Krug, D.; Kim, H.U.; Bruccoleri, R.; Medema, M.H. antiSMASH 3.0—a comprehensive resource for the genome mining of biosynthetic gene clusters. *Nucleic Acids Res.* **2015**, *43*, W237–W243. [CrossRef] [PubMed]
34. McArthur, A.G.; Waglechner, N.; Nizam, F.; Yan, A.; Azad, M.A.; Baylay, A.J.; Wright, G.D. The comprehensive antibiotic resistance database. *Antimicrob. Agents Chemother.* **2013**, *57*, 3348–3357. [CrossRef]
35. Cuppels, D.A.; Ainsworth, T. Molecular and physiological characterization of Pseudomonas syringae pv. tomato and Pseudomonas syringae pv. maculicola strains that produce the phytotoxin coronatine. *Appl. Environ. Microbiol.* **1995**, *61*, 3530–3536. [CrossRef]
36. Khusainov, I.; Fatkhullin, B.; Pellegrino, S.; Bikmullin, A.; Liu, W.; Gabdulkhakov, A.; Al Shebel, A.; Golubev, A.; Zeyer, D.; Trachtmann, N.; et al. Mechanism of ribosome shutdown by RsfS in Staphylococcus aureus revealed by integrative structural biology approach. *Nat. Commun.* **2020**, *11*, 1656. [CrossRef]
37. Egamberdieva, D.; Kamilova, F.; Validov, S.; Gafurova, L.; Kucharova, Z.; Lugtenberg, B. High incidence of plant growth-stimulating bacteria associated with the rhizosphere of wheat grown on salinated soil in Uzbekistan. *Environ. Microbiol.* **2008**, *10*, 1–9. [CrossRef]
38. Clinical and Laboratory Standard Institute (CLSI). *Performance Standards for Antimicrobial Susceptibility Testing*, 7th ed.; Sixteenth Informational Supplement; CLSI: Wayne, PA, USA, 2006; pp. 15–130.
39. Hadfield, J.; Croucher, N.J.; Goater, R.J.; Abudahab, K.; Aanensen, D.M.; Harris, S.R. Phandango: An Interactive Viewer for Bacterial Population Genomics. *Bioinformatics* **2018**, *34*, 292–293. [CrossRef]
40. Diabankana, R.G.C.; Shulga, E.U.; Validov, S.Z.; Afordoanyi, D.M. Genetic Characteristics and Enzymatic Activities of Bacillus velezensis KS04AU as a Stable Biocontrol Agent against Phytopathogens. *Int. J. Plant Biol.* **2022**, *13*, 201–222. [CrossRef]
41. Hussein, K.A.; Joo, J.H. Stimulation, purification, and chemical characterization of siderophores produced by the rhizospheric bacterial strain Pseudomonas putida. *Rhizosphere* **2017**, *4*, 16–21. [CrossRef]
42. Weimer, A.; Kohlstedt, M.; Volke, D.C.; Nikel, P.I.; Wittmann, C. Industrial biotechnology of Pseudomonas putida: Advances and prospects. *Appl. Microbiol. Biotechnol.* **2020**, *104*, 7745–7766. [CrossRef] [PubMed]
43. Loeschcke, A.; Thies, S. Pseudomonas putida—a versatile host for the production of natural products. *Appl. Microbiol. Biotechnol.* **2015**, *99*, 6197–6214. [CrossRef] [PubMed]
44. Zhang, S.; Ma, C.; Li, Q.; Li, Q.; He, Y.C. Efficient chemoenzymatic valorization of biobased D-fructose into 2, 5-bis (hydroxymethyl) furan with deep eutectic solvent Lactic acid: Betaine and Pseudomonas putida S12 whole cells. *Bioresour. Technol.* **2022**, *344*, 126299. [CrossRef] [PubMed]
45. Alonso-Campos, V.; Covarrubias-García, I.; Arriaga, S. Styrene bioconversion by Pseudomonas putida utilizing a non-aqueous phase for polyhydroxyalkanoate production. *J. Chem. Technol. Biotechnol.* **2022**, *97*, 1424–1435. [CrossRef]
46. Kuatsjah, E.; Johnson, C.W.; Salvachúa, D.; Werner, A.Z.; Zahn, M.; Szostkiewicz, C.J.; Singer, C.A.; Dominick, G.; Okekeogbu, I.; Haugen, S.J.; et al. Debottlenecking 4-hydroxybenzoate hydroxylation in Pseudomonas putida KT2440 improves muconate productivity from p-coumarate. *Metab. Eng.* **2022**, *70*, 31–42. [CrossRef]
47. Fernández, M.; Duque, E.; Pizarro-Tobías, P.; Van Dillewijn, P.; Wittich, R.M.; Ramos, J.L. Microbial responses to xenobiotic compounds. Identification of genes that allow Pseudomonas putida KT2440 to cope with 2, 4, 6-trinitrotoluene. *Microb. Biotechnol.* **2009**, *2*, 287–294. [CrossRef]
48. Thomassen, G.M.B.; Reiche, T.; Tennfjord, C.E.; Mehli, L. Antibiotic Resistance Properties among Pseudomonas spp. Associated with Salmon Processing Environments. *Microorganisms* **2022**, *10*, 1420. [CrossRef]
49. Igbinosa, I.H.; Nwodo, U.U.; Sosa, A.; Tom, M.; Okoh, A.I. Commensal Pseudomonas species isolated from wastewater and freshwater milieus in the Eastern Cape Province, South Africa, as reservoir of antibiotic resistant determinants. *Int. J. Environ. Health Res.* **2012**, *9*, 2537–2549. [CrossRef]
50. Rojas Murcia, N.; Lee, X.; Waridel, P.; Maspoli, A.; Imker, H.J.; Chai, T.; Walsh, C.T.; Reimmann, C. The Pseudomonas aeruginosa antimetabolite L-2-amino-4-methoxy-trans-3-butenoic acid (AMB) is made from glutamate and two alanine residues via a thiotemplate-linked tripeptide precursor. *Front. Microbiol.* **2015**, *6*, 170. [CrossRef]
51. McLeish, M.J.; Kneen, M.M.; Gopalakrishna, K.N.; Koo, C.W.; Babbitt, P.C.; Gerlt, J.A.; Kenyon, G.L. Identification and characterization of a mandelamide hydrolase and an NAD (P)+-dependent benzaldehyde dehydrogenase from Pseudomonas putida ATCC 12633. *J. Bacteriol.* **2003**, *185*, 2451–2456. [CrossRef]
52. Tiso, T.; Wierckx, N.; Blank, L.M. Non-pathogenic Pseudomonas as platform for industrial biocatalysis. *Ind. Biocatal.* **2014**, *1*, 323–372.
53. Jiang, W.; Marraffini, L.A. CRISPR-Cas: New tools for genetic manipulations from bacterial immunity systems. *Annu. Rev. Microbiol.* **2015**, *69*, 209–228. [CrossRef] [PubMed]
54. Maxwell, K.L. Phages fight back: Inactivation of the CRISPR-Cas bacterial immune system by anti-CRISPR proteins. *PLoS Pathogens* **2016**, *12*, e1005282. [CrossRef] [PubMed]
55. Cumby, N.; Davidson, A.R.; Maxwell, K.L. The moron comes of age. *Bacteriophage* **2012**, *2*, 5012–5019. [CrossRef]
56. Schroven, K.; Aertsen, A.; Lavigne, R. Bacteriophages as drivers of bacterial virulence and their potential for biotechnological exploitation. *FEMS Microbiol. Rev.* **2021**, *45*, fuaa041. [CrossRef]
57. Wang, X.; Kim, Y.; Ma, Q.; Hong, S.H.; Pokusaeva, K.; Sturino, J.M.; Wood, T.K. Cryptic prophages help bacteria cope with adverse environments. *Nat. Commun.* **2010**, *1*, 147. [CrossRef]

58. Nobrega, F.L.; Walinga, H.; Dutilh, B.E.; Brouns, S.J. Prophages are associated with extensive CRISPR–Cas auto-immunity. *Nucleic Acids Res.* **2020**, *48*, 12074–12084. [CrossRef]
59. Pleška, M.; Lang, M.; Refardt, D.; Levin, B.R.; Guet, C.C. Phage–host population dynamics promotes prophage acquisition in bacteria with innate immunity. *Nat. Ecol. Evol.* **2018**, *2*, 359–366. [CrossRef]